JOURNAL OF CATALYSIS 107, 535–547 (1987)

Effects of Oxidation/Reduction Treatments on the Morphology of Silica-Supported Rhodium Catalysts

CHOR WONG AND ROBERT W. MCCABE

Physical Chemistry Department, General Motors Research Laboratories, Warren, Michigan 48090-9055

Received October 27, 1986; revised April 28, 1987

The effects of oxidation, reduction, and alternating oxidation/reduction treatments on the oxidation state and the morphology of silica-supported Rh catalysts have been examined by temperature-programmed reduction and transmission electron microscopy. Oxidation of the catalyst leads to two forms of Rh oxide which are distinguished by different reduction temperatures. Microbeam electron diffraction identified these two species as a crystalline Rh_2O_3 and a disordered stoichiometric equivalent of Rh_2O_3. The disordered Rh_2O_3 is characterized by crystal domains less than 6.0 nm which can exist as segregated particles or as part of larger particles. The well-ordered crystalline Rh_2O_3 is associated with particles greater than 10.0 nm. The two forms of Rh_2O_3 can be interconverted—crystalline Rh_2O_3 formed by high-temperature oxidation can be converted to the disordered form by low-temperature reduction followed by a mild reoxidation. These observations support previous studies which suggest that the morphology of small Rh particles differs from that of large Rh particles. Moreover, our observations indicate that detailed characterization of the microstructure of supported Rh catalysts will be crucial to understanding their reduction, oxidation, and catalytic properties.

INTRODUCTION

There has been much recent interest in the catalytic properties of rhodium (*1–5*), particularly for automobile exhaust applications, where it is generally recognized that rhodium is the active component for both NO reduction and CO oxidation during lean-to-rich excursions (*1*). Despite the importance of Rh in automotive catalysis, questions remain concerning the manner in which Rh catalysts respond to changes in exhaust composition and temperature. Characterization of the supported rhodium is further complicated because it has several known stable oxidation states. In order to understand the effects of oxidation and reduction on catalyst performance, the oxidation state, dispersion, and the morphology of the supported Rh must be characterized.

Previous attempts to characterize supported rhodium catalysts have shown that the support plays a significant role in determining their activity and stability. Yao *et al.* (*2*) examined the effects of oxidation on Rh/Al_2O_3 catalysts by temperature-programmed reduction (TPR). They found that oxidation at 875 K led to two forms of rhodium which were reduced at different temperatures. The two forms of rhodium were attributed to a dispersed phase and a bulk-like three-dimensional phase. It was also observed that oxidations above 875 K produced a Rh oxide species that could not be accounted for in the subsequent reduction. It was suggested that at high temperatures the Rh oxide dissolved into the subsurface region of the Al_2O_3 support. Vis *et al.* (*3*) examined the morphologies of Rh/Al_2O_3 and Rh/TiO_2 by TPR and transmission electron microscopy. They concluded that dispersed Rh is the only species found on Al_2O_3. However, two forms of rhodium were found on TiO_2; it was suggested that these correspond to a raft-like dispersed form and a spherical bulk-like form. Del Angel *et al.* (*4*) examined the activity of Rh/Al_2O_3 and Rh/SiO_2 for methylcyclopentane hydrogenolysis. On SiO_2, small rho-

0021-9517/87 $3.00

dium particles exhibited greater specific activity than large rhodium particles. The reverse trend was observed on Al_2O_3 where large rhodium particles were more active. The variation of activity with rhodium dispersion was attributed to the ability of Al_2O_3 to stabilize the cubooctahedral morphology of Rh particles. On SiO_2, the Rh particles assumed the typical icosahedral morphology normally associated with supported FCC metals in the absence of such an interaction. The above results all indicate that the support plays a critical role in determining the activity of Rh catalysts. Interactions between the small Rh particles and the support can significantly affect the morphology and dispersion of supported Rh and ultimately affect the activity of the catalyst.

This study relates oxidation and reduction characteristics of silica-supported rhodium catalysts to their microstructure as determined by transmission electron microscopy and microbeam electron diffraction. SiO_2 was utilized as the support because of its minimal interaction with Rh, thus allowing us to examine the effects of oxidation and reduction treatments on small Rh particles in the absence of a strong metal–support interaction. This work thus provides a baseline for future work involving Rh supported on more strongly interacting supports such as alumina and modified aluminas; it should also allow the decoupling of effects related to small Rh particles alone from those involving interactions of Rh particles with the support.

EXPERIMENTAL PROCEDURE

Catalyst Preparation

The catalyst was prepared by impregnating a Davison 923 silica (100–200 mesh; BET area, 359 m^2/g) with a rhodium hexammine salt to produce a uniform 1% Rh distribution on the silica support. The catalyst was reduced in flowing 5% H_2/N_2 at 575 K for 2 h prior to use. H_2 chemisorption of the fresh (i.e., prereduced) catalyst yielded a Rh dispersion of 10% assuming one H atom per surface Rh atom.

Temperature-Programmed Reduction/ Oxidation

The temperature-programmed reduction/oxidation (TPR/TPO) technique has been described in detail elsewhere (*12*). Our apparatus, Fig. 1, utilizes thermal conductivity detectors to measure the uptake of either hydrogen or oxygen as the temperature of the catalyst is increased at a constant rate. The heating rate was 7 K/min in all experiments. Reductions of the catalyst were carried out in a 5% H_2/Ar mixture and oxidations were carried out in a 5% O_2/He mixture. Both the O_2/He and H_2/Ar were purified by passing through molecular sieve traps to remove any traces of water vapor prior to the first thermal conductivity detector; the hydrogen mixture was also passed through an oxygen trap. Mass flow controllers were used to maintain the flow rate of the gas mixtures at 10 std cc/min. Water vapor, produced by the reduction of metal oxide, was removed by a dry ice–acetone cold trap, filled with crushed high surface area alumina beads, downstream of the reactor. Experiments were typically performed with 0.250 g samples of the catalyst, which was sufficiently small to allow us to

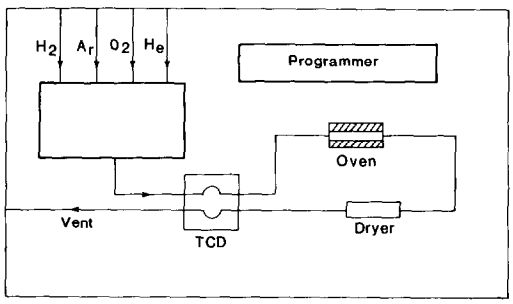

FIG. 1. A schematic diagram of the temperature-programmed reduction/oxidation (TPR/TPO) apparatus. Two thermal conductivity detectors were employed to measure differences in H_2 or O_2 concentrations across the reactor. Operating in the differential mode, the difference in H_2 or O_2 concentration is proportional to the rate of uptake by the sample.

operate the reactor in a differential mode and still measure differences in hydrogen uptake corresponding to 2% of the rhodium. The total uptake of hydrogen or oxygen was determined by integrating the area under the TPR or TPO profiles.

Transmission Electron Microscopy

Small samples of catalyst were withdrawn from the reactor after various treatments and subsequently examined by transmission electron microscopy (TEM) and X-ray diffraction (XRD). The TEM samples were crushed in a pestle and mortar, slurried with methanol, and deposited on a copper grid coated with a carbon film. The TEM grids were subsequently coated with a thin film of carbon in a vacuum coater to improve sample stability in the electron beam.

The samples were examined in a JOEL 100CX TEM/STEM at the University of Michigan. The Rh particle size distributions were obtained by measuring the diameters of approximately 400 particles from their corresponding electron micrographs. The dispersion of the fresh catalyst was calculated from the particle size distribution by assuming that the Rh particles were hemispherical. The dispersion thus obtained was in good agreement with hydrogen chemisorption results. Microbeam electron diffraction was utilized to examine the morphology of individual Rh particles. Diffraction patterns were obtained with the electron microscope operating in the STEM mode utilizing a 10.0-nm-diameter probe. Diffraction results from 15.0-nm-diameter areas of the catalyst could be obtained after accounting for beam broadening effects associated with the silica support.

RESULTS

Temperature-Programmed Reduction/ Oxidation

Typical oxidation profiles for the fresh, prereduced 1% Rh/SiO_2 catalyst and for bulk Rh powder are shown in Fig. 2. The

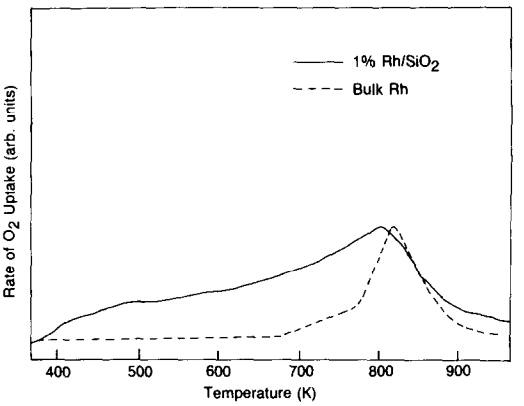

FIG. 2. Oxidation profile of 1% Rh/SiO_2 catalyst. The dashed curve is the oxidation profile for a 2.5-mg sample of bulk Rh powder.

supported rhodium oxidized much more readily at low temperatures than the bulk rhodium powder. As the supported sample was heated in O_2 above 675 K, a peak developed which was similar in shape and temperature to the corresponding peak for bulk rhodium. The combination of the broad low-temperature oxidation feature and the bulk-like oxidation feature suggests there is more than one form of rhodium on the supported catalyst.

Temperature-programmed reduction was used to further investigate the two forms of supported rhodium. Figure 3 shows TPR profiles obtained after the catalyst was oxidized to successively higher temperatures. The temperature ramp was held at the indicated temperatures for 1 h in the flowing 5% O_2/He feed. Partial oxidation of the catalyst to 673 K, just below the temperature where oxidation of bulk rhodium is initiated, produced only one peak (centered at 355 K) in the subsequent reduction profile. In comparison the reduction rate of bulk Rh_2O_3 peaked at 450 K as shown by the dashed curve in Fig. 3. The low-temperature TPO and TPR features associated with supported Rh indicate that there is an additional form of rhodium in the supported catalyst which is easier both to oxidize and reduce than bulk material.

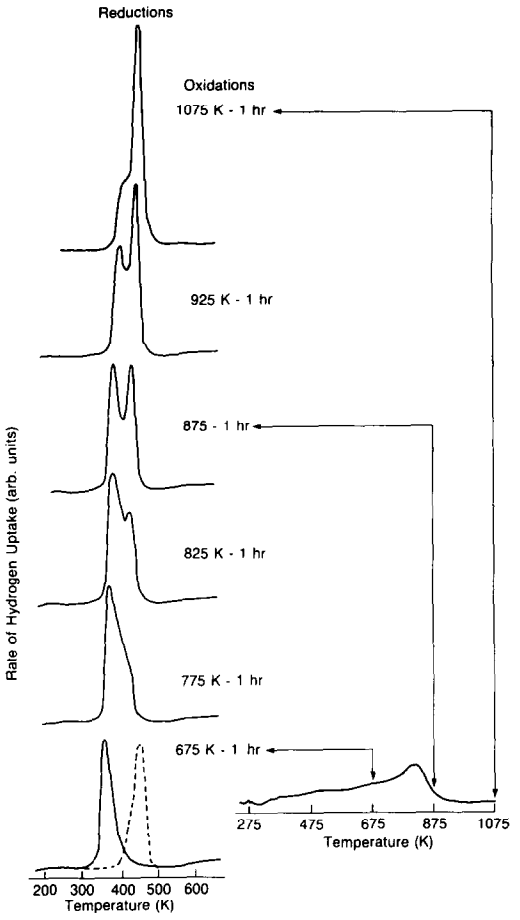

FIG. 3. Reduction profiles for 1% Rh/SiO_2 catalyst after oxidation to subsequently higher temperatures and holding for 1 h at the temperatures indicated. A typical oxidation profile is included in the inset. The dashed curve in the lowest reduction profile corresponds to the reduction of bulk Rh_2O_3.

Continued oxidation to temperatures greater than 675 K led to two peaks in the subsequent reduction profiles in Fig. 3—an easy-to-reduce form which corresponds to the low-temperature feature during oxidation and a bulk-like form of Rh oxide which corresponds to the high-temperature feature during oxidation. Oxidation was complete by 875 K as shown in Fig. 4a where the total hydrogen uptake is plotted as a function of oxidation temperature. Furthermore, upon complete oxidation, the subsequent overall reduction stoichiometry corresponded to the reduction of Rh_2O_3 to Rh metal. Continued heating at higher temperatures shifted rhodium oxide from the easy-to-reduce form to the bulk-like form without affecting the total hydrogen uptake. This is shown in Fig. 4b where the fraction of rhodium in the easily reduced form is plotted as a function of oxidation temperature.

The shift in rhodium from one form to another is reversible; the low-temperature reduction peak could be restored in a severely oxidized catalyst by a mild reduction which was just sufficient to reduce all of the rhodium back to the metallic state. Figure 5 illustrates such an experiment. A fresh catalyst was initially oxidized to 1075 K for 2 h to shift most of the Rh into the bulk Rh_2O_3 state. The corresponding oxidation profile is shown in Fig. 5A. After the severe oxidation to 1075 K, the catalyst was subjected to a mild but complete reduction to 475 K as shown in Fig. 5B. The reduction profile verified that the 1075 K oxidation had converted most of the Rh oxide to the bulk Rh_2O_3 form. Despite this conversion, the oxidation profile, obtained following the 475 K reduction (Fig. 5C), resembled that of the fresh catalyst. The fraction of oxygen uptake under the broad low-temperature oxidation peak was nearly equivalent to that of the fresh catalyst, indicating that the mild reduction had returned the catalyst to a nearly fresh state. This observation was confirmed by the subsequent reduction profile, Fig. 5D, which showed that most of the rhodium oxide was in the easy-to-reduce form.

Analysis by X-ray diffraction showed that Rh_2O_3 and Rh metal were the only species detected on the oxidized and reduced samples, respectively. Transmission electron microscopy was employed to characterize the two forms of rhodium in further detail. These results will be discussed in the next section.

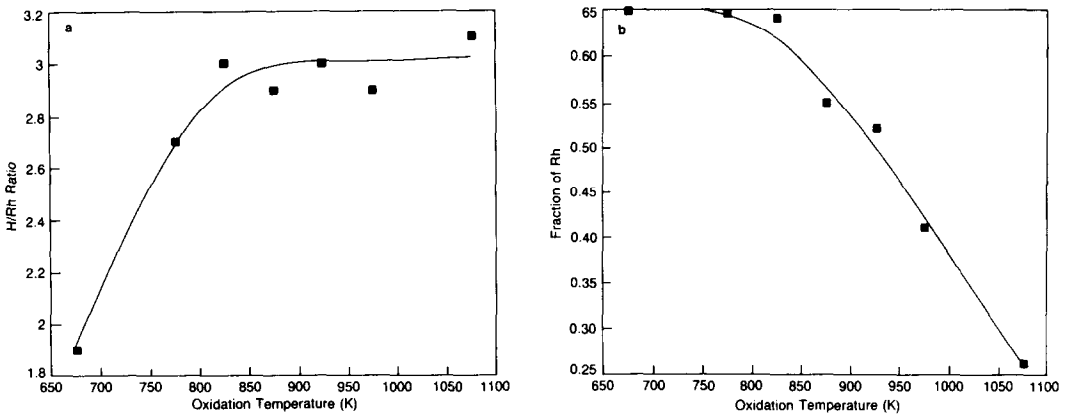

FIG. 4. (a) The dependence of total hydrogen uptake, in the reduction of 1% Rh/SiO_2 catalyst, on the final temperature of oxidation. The final temperature was maintained for 1 h in all cases. (b) A plot of the corresponding fraction of Rh oxide in the low-temperature reducible state of the catalyst as a function of the oxidation temperature for the catalyst shown in (a).

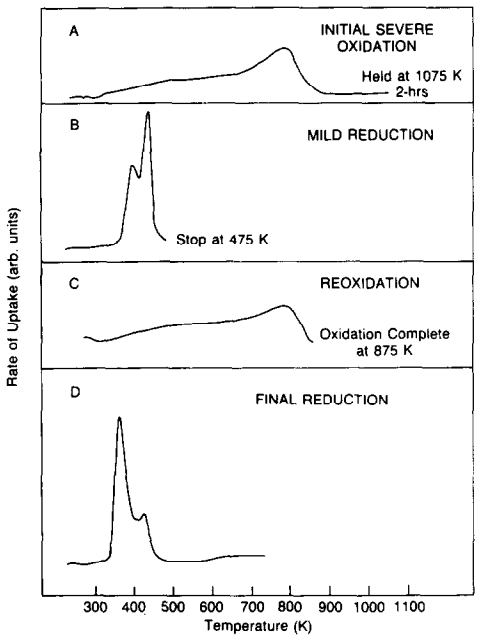

FIG. 5. An illustration of an experiment that regenerates the low-temperature reduction peak of the catalyst. (A) Oxidation of a fresh catalyst sample to 1075 K/2 h. (B) Complete reduction of the catalyst in (A) to 475 K. (C) Subsequent reoxidation of the catalyst to 875 K (note the similarity between (C) and the oxidation profile for fresh catalyst in (A)). (D) Final reduction profile of the catalyst after complete oxidation at 875 K. Note that the majority of the Rh oxide is now in the low-temperature reduction peak.

Transmission Electron Microscopy

Figure 6 shows representative micrographs and particle size distributions for a 1% Rh/SiO_2 catalyst after various treatments. In the fresh catalyst (Fig. 6a) over 85% of all rhodium particles examined were between 2.0 and 6.0 nm in diameter. Figure 6b shows a sample which was oxidized at 1075 K for 2 h. This high-temperature-oxidized (HTO) catalyst had a significantly larger mean particle diameter than the fresh sample; the majority of the Rh oxide particles were between 10.0 and 14.0 nm in diameter. The distribution was also significantly broader than that in the fresh catalyst, showing that the population of large particles had increased as the population of small particles decreased. Comparison of the TPR profile and particle size distribution of the HTO sample with those of the fresh sample would suggest that the low-temperature TPR peak is associated with particles of 6.0 nm or less in diameter while the high-temperature TPR peak is associated with particles of 12.0 nm or greater diameter. However, when the HTO sample was reduced at 475 K, the particle size distribution (Fig. 6c) did not change signif-

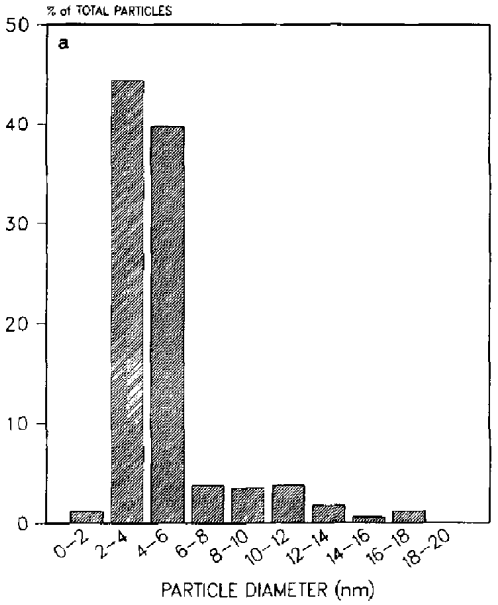

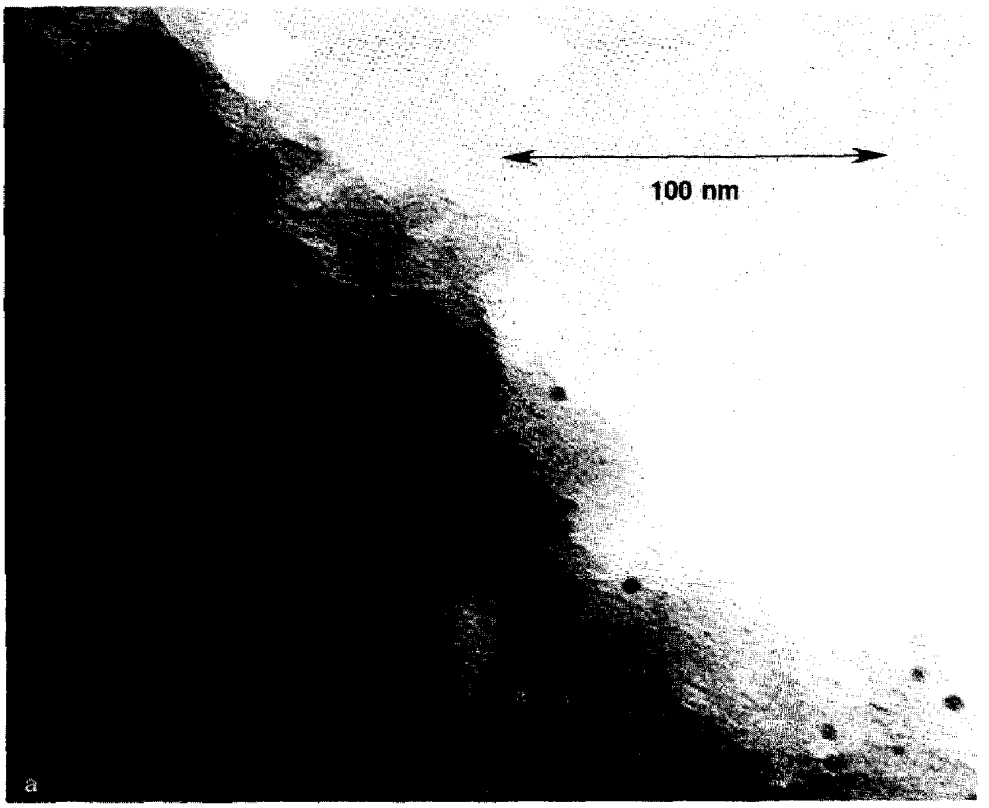

FIG. 6. (a) Electron micrograph of the fresh catalyst with its corresponding Rh particle size distribution. (b) Electron micrograph of the catalyst after oxidation to 1075 K for 2 h, with corresponding particle size distribution. (c) Electron micrograph after mild reduction of catalyst in (b) with corresponding particle size distribution.

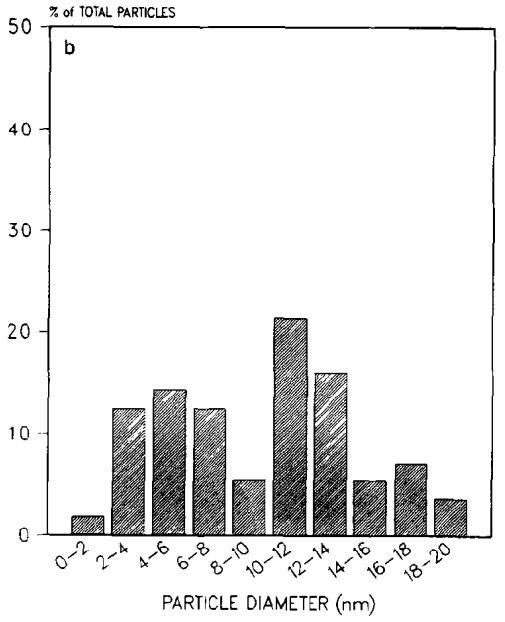

FIG. 6—*Continued.*

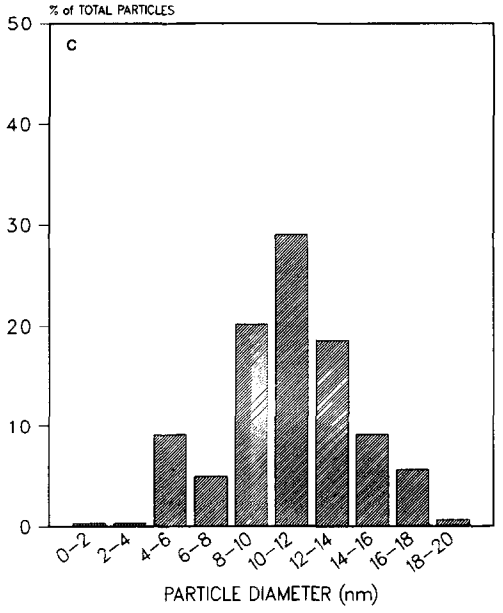

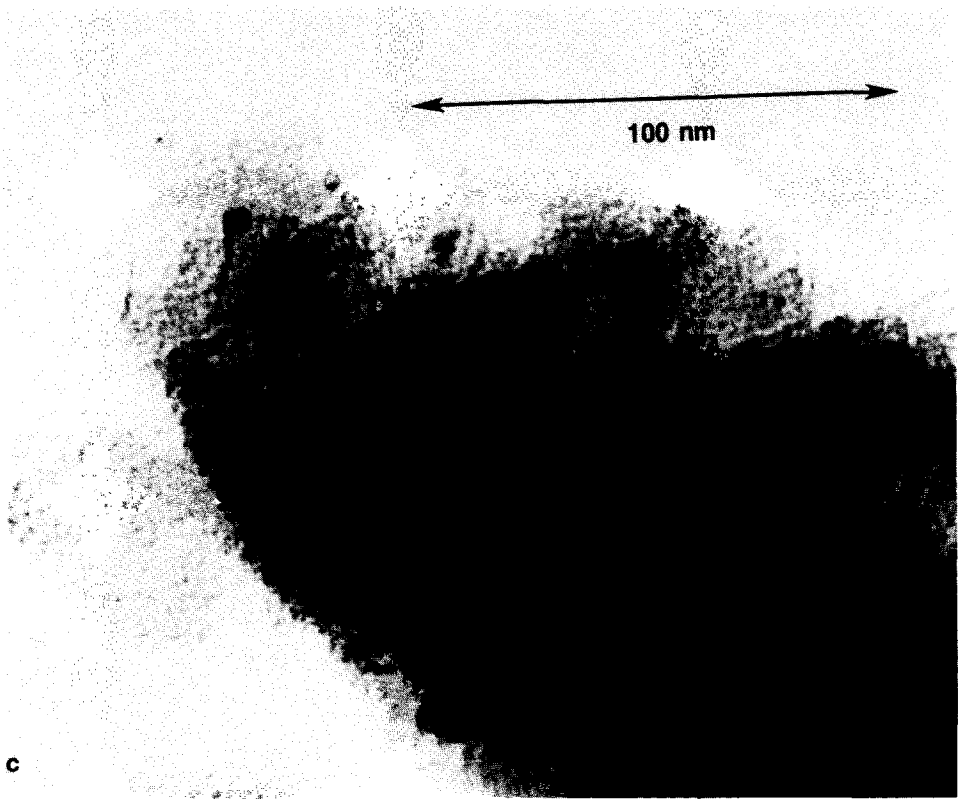

FIG. 6—*Continued.*

icantly despite reversion of the subsequent TPO and TPR profiles back to those nearly characteristic of the fresh catalyst. This indicates that a high-temperature oxidation followed by a low-temperature reduction produces changes in the supported Rh catalyst which cannot be ascribed simply to changes in gross particle dimensions as observed by bright field transmission electron microscopy.

X-ray diffraction of the bulk catalyst and microbeam electron diffraction in the TEM were employed to further examine the morphology of the catalyst after oxidation and reduction treatments. The bulk XRD data simply confirmed the presence of Rh_2O_3 in the oxidized sample and Rh metal in the reduced sample. No other crystalline forms of Rh were observed and no information could be gained concerning the degree of crystallinity of the Rh and the Rh_2O_3 particles. However, microbeam electron diffraction enabled us to obtain further insight into the structure of individual crystallites. A microbeam electron diffraction pattern from a single 10.0-nm particle of a catalyst oxidized at 875 K for 8 h is shown in Fig. 7a. The pattern consists of "spotty rings" which indicates that the crystallites of the samples are small and not well-aligned. In contrast, the diffraction pattern for a sample oxidized at 1075 K for 2 h, Fig. 7b, showed distinct higher index spots which correspond to the expected pattern for a hexagonal close-packed Rh_2O_3 lattice viewed along the (0001) zone axis. However, the spots near the center of the pattern are split and are not in their predicted equilibrium positions for a hexagonal close-packed structure. This indicates that the rhodium oxide particle still has not attained a fully single crystal Rh_2O_3

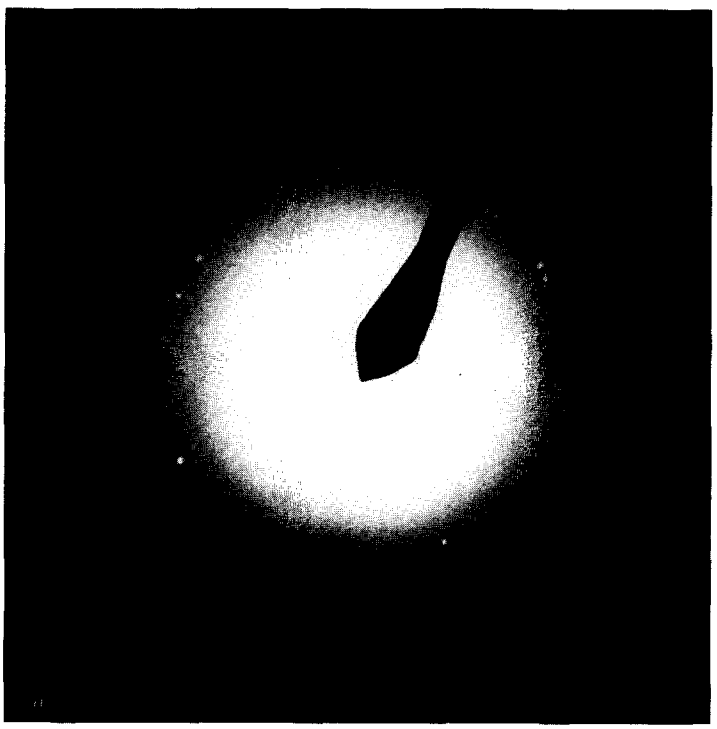

FIG. 7. (a) Microbeam electron diffraction pattern of a typical Rh oxide particle after oxidation at 875 K for 8 h. (b) Microbeam electron diffraction pattern of a typical Rh oxide particle after oxidation at 1075 K for 2 h. (c) Microbeam electron diffraction pattern of a Rh particle after oxidation at 1075 K for 2 h followed by a complete reduction by heating briefly to 475 K in 5% H_2/Ar.

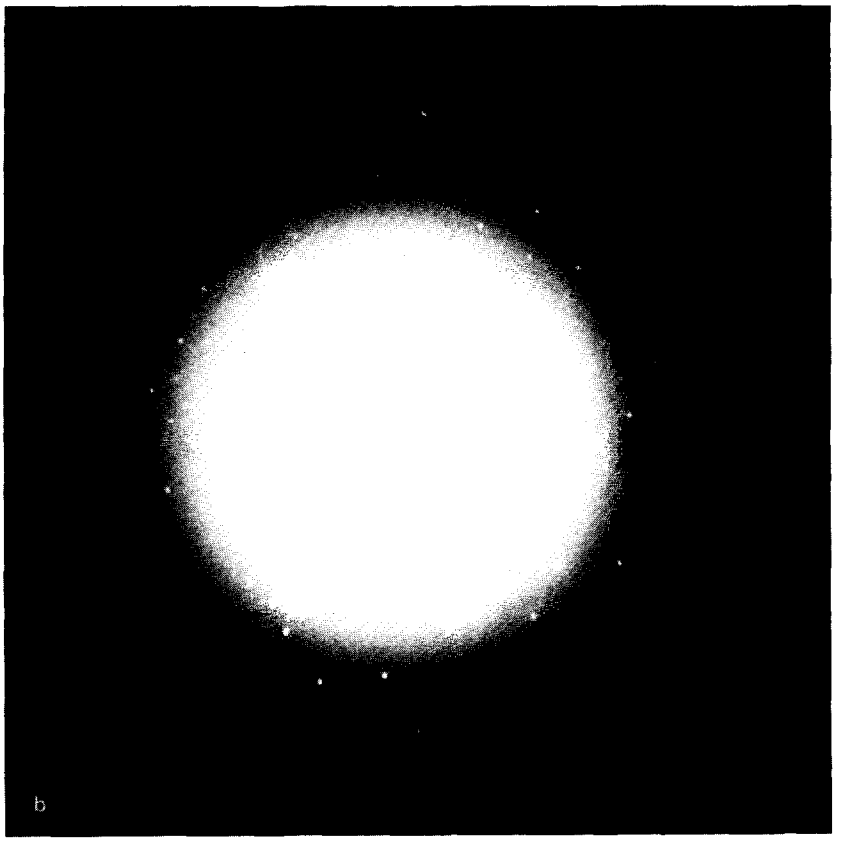

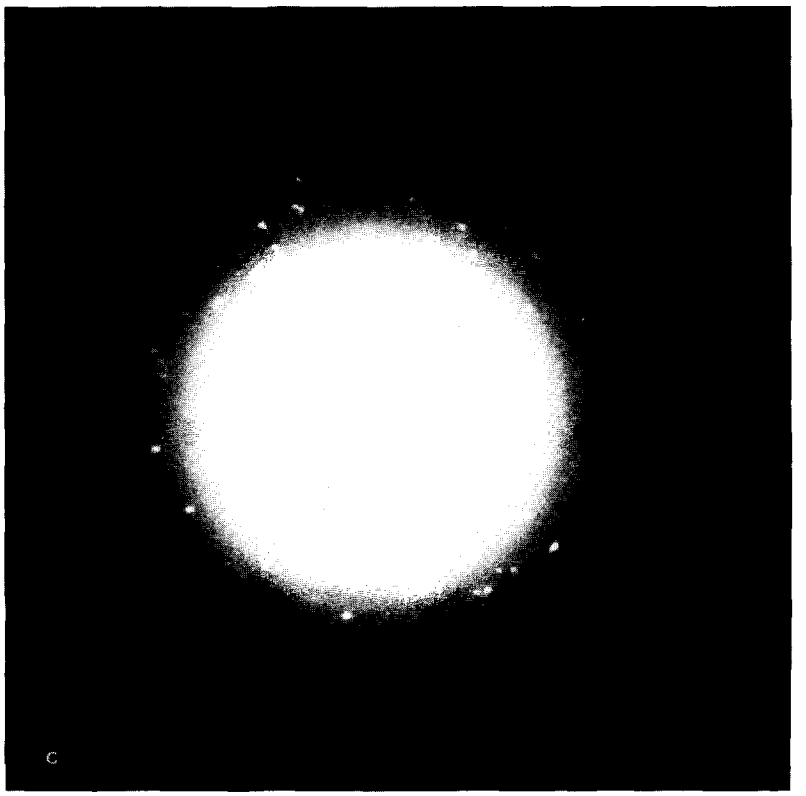

FIG. 7—*Continued.*

structure even after extensive oxidation at 1075 K.

Reduction of the catalyst in Fig. 7b at 475 K produces the microbeam electron diffraction pattern in Fig. 7c which does not correspond to a pattern from the face centered cubic rhodium lattice. The resulting diffraction pattern is that of a spotty ring, which indicates that the resulting rhodium particle is an aggregate of small crystallites. The microbeam electron diffraction patterns and images clearly show that oxidation produces a fine grain Rh_2O_3, which forms bulk-like crystals only after continued exposure to oxygen at high temperatures.

DISCUSSION

The dependence of the TPR profile on the oxidation temperature indicates that high-temperature oxidation continues to change the catalyst even though the rhodium has been completely oxidized to the stoichiometric equivalent of Rh_2O_3 by 875 K. Microbeam electron diffraction shows that oxidation at 875 K produces a disordered Rh oxide. Only after continued oxidation at higher temperatures can crystalline Rh_2O_3 be obtained. The two peaks in the subsequent reduction profile result from the disordered Rh_2O_3 fraction reducing at lower temperatures than the bulk-like crystalline fraction. The decrease in the low-temperature reduction peak with increasing oxidation temperature is consistent with the formation of crystalline Rh_2O_3 at high temperatures and is confirmed by microbeam electron diffraction. Reduction of the Rh_2O_3 to Rh metal at 475 K produced Rh particles which were aggregates of small crystallites. The breakdown of order in the Rh lattice suggests that reduction did not occur under equilibrium conditions. These results are consistent with the observations of Wang and Schmidt (7) for Rh supported on thin film SiO_2. They showed that oxidation at 825 K followed by reduction at 675 K resulted in the formation of cracks and fissures in the Rh particles. Our results indicate similar changes, as shown, for example, in Fig. 8, which is a micrograph of the Rh/SiO_2 catalyst after a treatment involving oxidation at 875 K followed by reduction at 675 K. The Rh particles on the edge of the silica appear to have split into smaller, contiguous particles. These results indicate that the morphology of the Rh is sensitive to oxidation/reduction treatments. The dependence of catalyst morphology on oxidation/reduction treatments has implications for the lean-to-rich operation in automotive catalysis. During such transients, the alternating oxidizing and reducing environments will continually change the morphology of the catalyst.

The changes in ethane hydrogenolysis activity that accompany oxidation/reduction cycles have been examined by Lee and Schmidt (*13*) for a Rh/SiO_2 catalyst. The activity of the catalyst increased by three orders of magnitude while the Rh surface area increased only three times after an oxidation at 875 K followed by reduction at 475 K. The discrepancy between the increase in Rh dispersion and the disproportionately large increase in hydrogenolysis activity was attributed to a change in catalyst morphology as observed by TEM. Yates and Sinfelt (*5*) also examined ethane hydrogenolysis over a Rh/SiO_2 catalyst and observed a maximum in the specific activity when the Rh crystallite size was below 4.0 nm. The same dependence of activity on particle size was observed by Fuentes and Figueras (*6*) for cyclopentane hydrogenolysis, also a structure-sensitive reaction, on Rh/Al_2O_3 catalysts. All of these groups concluded that the morphology of highly dispersed Rh particles differed significantly from that of larger particles. Recent results from high-resolution electron microscopy (*8–11, 14*) have shown that highly dispersed FCC metals, such as Rh, do not adopt a single crystal morphology when the particle diameters are less than 10.0 nm; instead the metal assumes a multiply twinned structure. Furthermore it has also been observed that these multiply

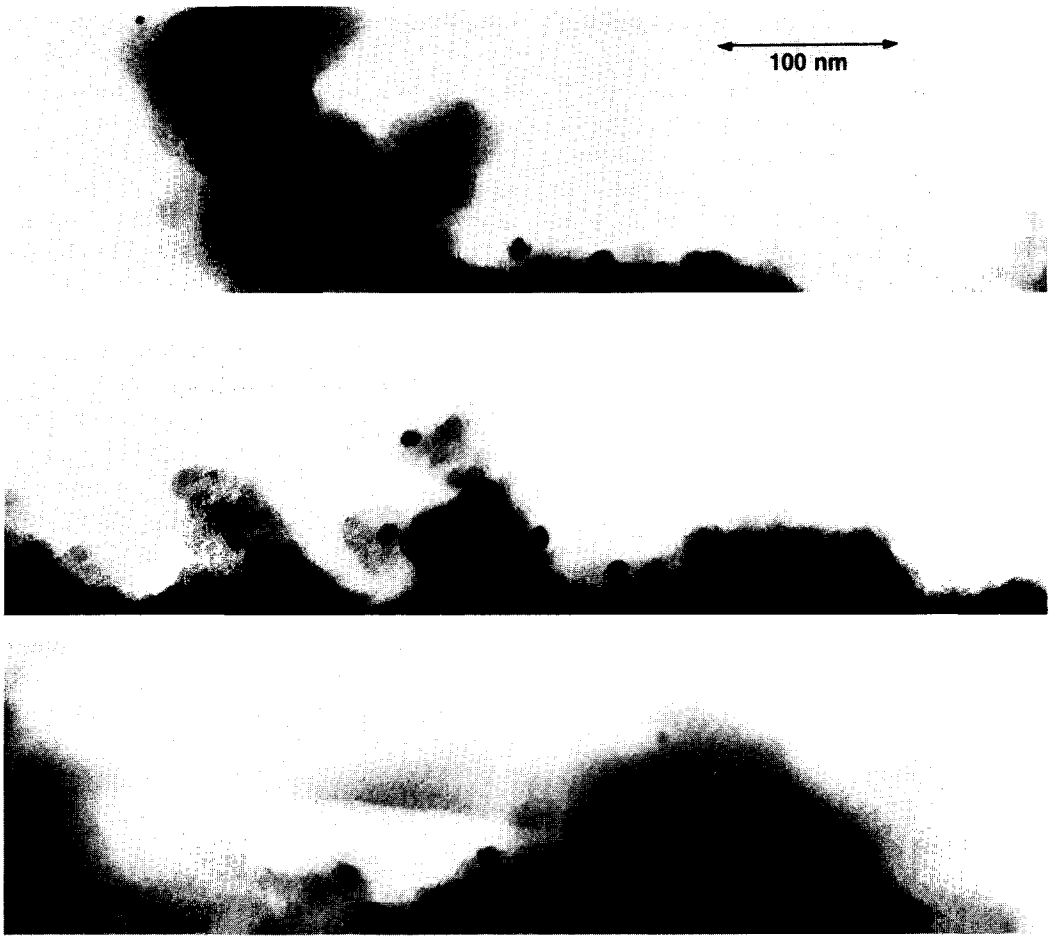

FIG. 8. Electron micrograph of selected areas of a catalyst oxidized at 875 K and reduced at 475 K. The particles on the edge of the silica are split as a result of the oxidation/reduction treatment.

twinned structures are only stable for particles with diameters less than 10.0 nm. Our TPR and microbeam electron diffraction results suggest that the crystallites produced by oxidation followed by reduction are less than 10.0 nm. For example, the particles shown in Fig. 8 are approximately 10.0 nm in overall diameter and contain multiple nuclei each of which is approximately 4.0–5.0 nm in diameter. The detailed structure of these nuclei are not well-known; however, their size and symmetry suggest that they have adopted a multiply twinned structure.

The TPR, TPO, and electron microscopy data show that alternating oxidation/reduction treatments can significantly alter the morphology of supported Rh catalysts. Rh particles ca 6.0 nm or less both oxidize and reduce more readily than larger particles. Moreover, the small particles need not be isolated on the support. They may exist as aggregates of small crystallites with overall diameters greater than 10.0 nm. These results, together with the reactivity data from the literature, demonstrate that detailed microstructural characterization is required to understand the reduction, oxidation, and catalytic properties of supported Rh. Simple particle size characterization, employing chemisorption techniques or gross particle size distribu-

tions by TEM, cannot be expected to correlate with reduction, oxidation, and catalytic properties.

SUMMARY AND CONCLUSIONS

- A 1% Rh/SiO_2 catalyst can be oxidized completely to Rh_2O_3 by heating in flowing 5% O_2/He to 875 K.
- Reduction of the oxidized catalyst to Rh metal can be effected by briefly heating to 475 K in flowing 5% H_2/Ar.
- Rh^0 and Rh^{3+} were the only oxidation states observed by both bulk X-ray diffraction and microbeam electron diffraction in the electron microscope.
- Temperature-programmed oxidation and temperature-programmed reduction experiments both show evidence for two forms of Rh in a 1% Rh/SiO_2 catalyst—a low-temperature oxidized/reduced form and a high-temperature oxidized/reduced form which resembles bulk Rh in its oxidation/reduction behavior.
- The two forms of Rh are distinguished by their particle morphology. The low-temperature reduction form is associated with particles with crystal domains ca. 6.0 nm or less which can exist either as segregated particles or as subunits of larger aggregates of crystallites. The high-temperature reduction form is associated with particles greater than 6.0 nm which exhibit a high degree of crystallinity in microbeam electron diffraction.
- Interconversion between the two forms occurs readily in alternating oxidizing/reducing environments at relatively low temperatures and results in nonequilibrium particle morphology.

ACKNOWLEDGMENTS

We thank Michael J. D'Aniello, Jr. and Michael G. Zammit for the preparation of the catalyst and also thank Professor L. D. Schmidt for helpful discussions. The assistance of Hildegard Hoonke of the Material Science Department at the University of Michigan was much appreciated in obtaining the TEM data.

REFERENCES

1. Schlatter, J. C., and Mitchell, P. J., *Ind. Eng. Chem. Prod. Res. Dev.* **19,** 288 (1980).
2. Yao, H. C., Japar, S., and Shelef, M., *J. Catal.* **50,** 407 (1977).
3. Vis, J. C., van't Blik, H. F. J., Huizinga, Y., van Grondelle, J., and Prins, R., *J. Catal.* **95,** 333 (1985).
4. del Angel, G., Coq, B., and Figueras, F., *in* "Metal-Support and Metal Additive Effects in Catalysis" (B. Imelik *et al.*, Eds.). Elsevier, Amsterdam, 1982.
5. Yates, D. J. C., and Sinfelt, J. H., *J. Catal.* **8,** 348 (1967).
6. Fuentes, S., and Figueras, F., *J. Catal.* **61,** 443 (1980).
7. Wang, T., and Schmidt, L. D., *J. Catal.* **70,** 187 (1981).
8. Avery, N. R., and Sanders, J. V., *J. Catal.* **18,** 129 (1970).
9. Marks, L. D., and Howie, A., *Nature (London)* **282,** 196 (1979).
10. Marks, L. D., *Ultramicroscopy* **18,** 445 (1985).
11. Iijima, S., and Ichihashi, T., *Phys. Rev. Lett.* **56,** 616 (1986).
12. Hurst, N. W., Gentry, S. J., Jones, A., and McNicol, B. D., *Catal. Rev. Sci. Eng.* **24,** 233 (1982).
13. Lee, C., and Schmidt, L. D., *J. Catal.* **101,** 123 (1986).
14. Yacaman, M. J., *Appl. Catal.* **13,** 1 (1984).